A FIRST LOOK AT THE DAMOCLOIDS

DAVID JEWITT[1]

Institute for Astronomy, University of Hawaii, 2680 Woodlawn Drive, Honolulu, HI 96822; jewitt@ifa.hawaii.edu

ABSTRACT

The Damocloids are objects thought, on dynamical grounds, to be inactive Halley-family and long-period comets. We present optical measurements of 12 such objects, finding that their mean Kron-Cousins colors are $B-V = 0.79 \pm 0.01$, $V-R = 0.48 \pm 0.01$, and $R-I = 0.48 \pm 0.01$. The normalized reflectivity spectra are generally linear, with a mean gradient $S' = 11.9\% \pm 1.0\%$ per 1000 Å. The latter is consistent with the mean $S' = 11.6\% \pm 2.3\%$ per 1000 Å measured for the nuclei of (short-period) Jupiter-family comets, a surprising result given the expected very different formation locations and dynamical histories of these two types of body. The Damocloids are devoid of the ultrared matter (with $S' \geq 25\%$ per 1000 Å) that is present on many Kuiper belt objects and Centaurs, and the mean colors of the Damocloids are inconsistent with those of the Kuiper belt objects ($S' = 21.1\% \pm 1.4\%$ per 1000 Å). The data suggest that the ultrared matter, widely thought to consist of a complex organic compound processed by prolonged exposure to cosmic rays, cannot survive long in the inner solar system. Timescales for ejection or burial of ultrared matter on the nuclei of both Jupiter-family comets and Damocloids are short. Such material may also be chemically unstable to the higher temperatures experienced in the inner planetary region.

Key words: comets: general — Kuiper belt — minor planets, asteroids

1. SCIENTIFIC MOTIVATION AND THE DAMOCLOID SAMPLE

The nuclei of comets are scientifically interesting as likely carriers of volatile and other material captured ~4.6 Gyr ago in the protoplanetary disk of the Sun. Unfortunately, because of their small size and the presence of near-nucleus coma when near perihelion (and thus at their brightest), cometary nuclei have also proved to be among the most difficult objects to study using astronomical techniques. Despite substantial observational efforts over the past two decades, the number of nuclei that are well characterized in terms of reliable measurements of their shapes, sizes, colors, albedos and spin states is only of order 10 (Campins & Fernández 2003; Lamy et al. 2004), although partial information is available for a larger number. Almost all of the well-observed nuclei are members of the short-period Jupiter-family comet (JFC) class. The JFCs are thought to have a source beyond Neptune within the Kuiper belt (from roughly 30 to 50 AU), although the precise location of the source remains unclear. The nuclei of the so-called long-period or "nearly isotropic" comets are observationally undersampled, in part because their strong mass-loss rates and bright comae typically swamp the light scattered from the nucleus.

The formation locations and dynamical histories of the long-period comets are likely different from those of the better studied JFCs. Most long-period comets probably formed not in the Kuiper belt but in the vicinity of the giant planets at 5 to 30 AU, where equilibrium temperatures were in the ~50 to ~150 K range. They were scattered out of the planetary region during near-miss interactions with the growing planets, and the perihelia of some (maybe ~10%) were lifted by the extragalactic tide and by random perturbations from passing stars,

producing the Oort cloud (Duncan et al. 1987). The suggestion by Fernández et al. (2003) that about 1% of the Oort cloud comets might be former members of the Kuiper belt's scattered-disk population does not materially change this scenario. Once in the Oort cloud, comets fall to equilibrium temperatures of ~10 K or less, suffer no collisions, and are subject to the full flux of ionizing cosmic radiation. In these respects they differ from comets originating in the Kuiper belt, which have radiation equilibrium temperatures near ~40 K, suffer collisions (indeed, the observed JFC nuclei may be produced by fragmentation of larger Kuiper belt objects; Farinella & Davis 1996), and are partially protected from cosmic rays by the heliosphere. It is interesting to ask whether different formation locations and processing histories might have led to measurable differences in the properties of cometary nuclei from Kuiper belt and Oort cloud sources.

In this paper, we begin to address this question using a set of objects known informally as Damocloids. Damocloids are solar system objects with orbits like those of Halley-family and long-period comets but without visible signs of outgassing. Like the archetypal object (5335) Damocles, their high eccentricities and inclinations suggest that the Damocloids are the dead or dormant nuclei of long-period comets (Asher et al. 1994). With no likely source in the Kuiper belt, the Damocloids constitute a sample from which the physical properties of long-period comet nuclei might be determined. Owing to the small number of known Damocloids and to their general faintness, no systematic study of these objects has yet been published, although a few detailed studies of particular objects exist (Davies et al. 1998, 2001; Harris et al. 2001; Fernández et al. 2001).

The Tisserand parameter, T_J, which is a constant of the motion in the restricted circular three-body problem, provides a useful metric with which to identify Damocloids. The parameter relative to Jupiter is defined by

$$T_J = \frac{a_J}{a} + 2\left[(1-e^2)\frac{a}{a_J}\right]^{1/2} \cos i, \qquad (1)$$

TABLE 1
CURRENTLY KNOWN DAMOCLOIDS

Name	a[a] (AU)	e[b]	i[c] (deg)	q[d] (AU)	T_J[e]
20461 Dioretsa (1999 LD_{31})	23.777	0.900	160.4	2.390	−1.542
2000 HE_{46}..................................	23.985	0.902	158.38	2.355	−1.508
1999 LE_{31}..................................	8.163	0.472	151.88	4.310	−1.310
C/LINEAR (2002 CE_{10})[f]............	9.816	0.791	145.46	2.047	−0.853
(65407) 2002 RP_{120}.....................	55.940	0.956	119.11	2.473	−0.845
2000 DG_8....................................	10.786	0.793	129.43	2.231	−0.631
C/LONEOS (2001 OG_{108})[f]	13.30	0.925	80.26	0.994	0.597
2000 AB_{229}................................	52.497	0.956	68.72	2.292	0.773
1997 MD_{10}.................................	26.740	0.942	59.04	1.543	0.975
C/LINEAR (2002 VQ_{94})[f]	218.161	0.969	70.50	6.800	1.095
5335 Damocles (1991 DA)	11.834	0.867	62.10	1.573	1.143
2002 XU_{93}.................................	67.426	0.689	77.88	20.983	1.173
1998 WU_{24}.................................	15.221	0.907	42.56	1.419	1.404
1999 XS_{35}	18.079	0.948	19.47	0.948	1.411
2000 KP_{65}	88.323	0.963	45.62	3.274	1.613
1996 PW	287.127	0.991	29.76	2.547	1.732
2003 WG_{166}	5.160	0.644	55.41	1.838	1.873
2003 WN_{188}	14.566	0.849	26.94	2.200	1.933
(15504) 1999 RG_{33}.....................	9.634	0.775	35.13	2.164	1.946
2004 DA_{62}	7.709	0.467	52.23	4.107	1.993

NOTE.—As of 2004 July 1. Objects are ordered by Tisserand parameter,
[a] Orbital semimajor axis.
[b] Orbital eccentricity.
[c] Orbital inclination.
[d] Perihelion distance.
[e] Tisserand parameter.
[f] These objects satisfied the working definition of Damocloids at discovery but were later observed to possess faint comae.

where a, e, and i are the semimajor axis, eccentricity, and inclination of the orbit while $a_J = 5.2$ AU is the semimajor axis of the orbit of Jupiter. For reference, the Halley-family comets (HFCs) have $T_J \leq 2$ and the JFCs have $2 < T_J \leq 3$, while most asteroids have $T_J > 3$. The Tisserand parameter is an imperfect metric in the sense that Jupiter's orbit is not a circle and the gravitational influences of other planets cannot in general be neglected in the calculation of long-term motions. Nevertheless, T_J provides a simple and revealing way to dynamically classify interplanetary objects (Carusi et al. 1995).

We define Damocloids as point-source objects having $T_J \leq 2$. With this definition, a search of the orbital elements database for asteroids maintained at the Lowell Observatory yields 20 Damocloids, which we list in order of T_J in Table 1. So defined, the Damocloids exhibit a wide range of orbital properties but are noteworthy for their high orbital eccentricities and inclinations. Six of the objects in Table 1 are retrograde ($i \geq 90°$), unlike any other class of asteroid or the JFCs, but consistent with the existence of retrograde long-period comets. Indeed, the cumulative distribution of the orbital inclinations of the Damocloids is consistent with that of the HFCs (Fig. 1), as would be expected if the former are physically evolved versions of the latter (Asher et al. 1994). The distribution of the inclinations of the JFCs is quite different (Fig. 1). Could the Damocloids be former JFCs that have dynamically evolved into HFC-like orbits? Numerical simulations suggest that this is unlikely (Levison & Duncan 1997). While some JFCs can, on long timescales, evolve across the $T_J = 2$ dividing line between the two populations, these objects tend to retain T_J close to 2. For example, only 2% of such bodies in Levison & Duncan's models have $T_J \leq 1$, whereas about 50% of the

Damocloids in Table 1 satisfy this condition. Therefore, we conclude that while it is possible that the sample may be weakly contaminated by highly dynamically evolved, inactive nuclei of JFCs (particularly for objects with $T_J \approx 2$), most Damocloids are unrelated to the JFCs.

As discussed below, some objects identified as Damocloids on the basis of their Tisserand parameters and asteroidal appearance have subsequently been found to display weak comae. This provides clear evidence that our simple, dynamical definition of the Damocloids picks out objects that are volatile-rich and, therefore, of a cometary nature. The coma in these objects is generally weak enough that scattered light from the nucleus dominates the observations. Weissman & Levison (1997) have argued that Damocloid 1996 PW could have an origin in the main asteroid belt. The stochastic nature of solar system dynamics makes it impossible to determine the origin of any particular object with absolute confidence, but the comet-like inclination distribution (Fig. 1) and the postdiscovery identification of coma in some Damocloids leaves little doubt that the sample in Table 1 consists predominantly of inactive comets.

2. OBSERVATIONS

Observations were taken at the University of Hawaii (UH) 2.2 m diameter telescope and the 10 m Keck I Telescope, both located on Mauna Kea in Hawaii. We worked at the f/10 Cassegrain focus of the UH 2.2 m using a Tektronix 2048 × 2048 pixel CCD camera and the "OPTIC" CCD camera, which contains two CCDs each 2048 × 4104 pixels in size. The Tektronix is a standard back-illuminated device antireflection-coated to provide ~90% quantum efficiency at wavelengths
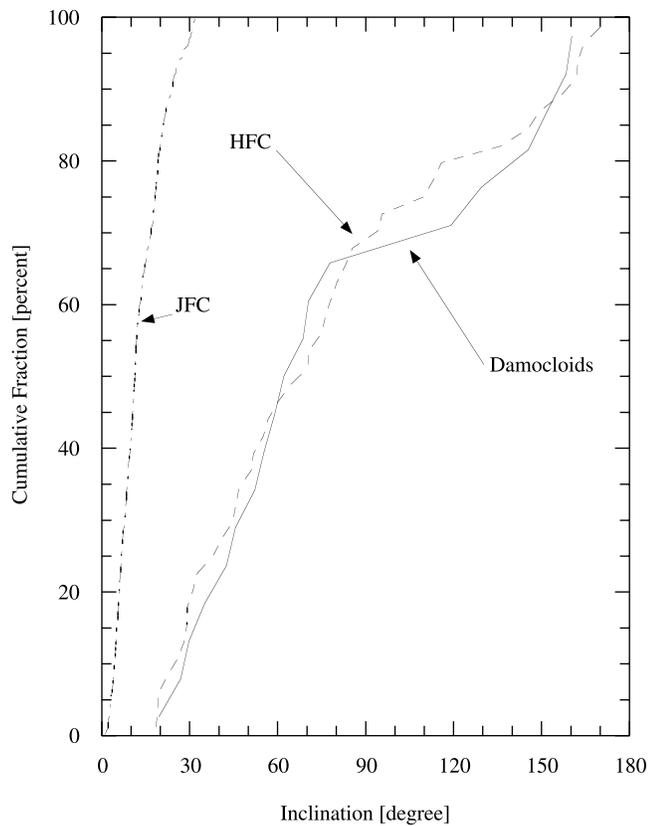
Fig. 1.—Cumulative distribution of the inclinations of the Damocloids (*solid curve*) compared with the Halley-family Comets (*dashed curve*) and Jupiter-family comets (*dash-dotted curve*), showing the great similarity between the Damocloids and the HFCs. The Damocloid sample consists of 20 point-source objects with $T_J \leq 2$, as discussed in § 1. The HFC and JFC samples consist of 42 comets with $T_J \leq 2$ and periods over 200 yr and 240 comets with $2 < T_J \leq 3$, respectively.

$\lambda \sim 0.7 \ \mu$m. OPTIC is an orthogonal transfer CCD, in which charge packets can be moved on the detector during the integration in order to provide tip-tilt corrections to the wave front (Tonry et al. 1997). This results in a net improvement in the image quality. Image scales from the Tektronix and OPTIC cameras were $0\rlap{.}''22$ pixel^{-1} and $0\rlap{.}''14$ pixel^{-1}, respectively. OPTIC was read out with the pixels binned 2×2 while maintaining Nyquist sampling of the telescope point-spread function. At Keck we used the LRIS camera (Oke et al. 1995), equipped with another Tektronix 2048×2048 pixel CCD. The image scale was $0\rlap{.}''22$ pixel^{-1}.

The objects were identified by their distinctive motions relative to the fixed stars. Observations were taken with the telescopes tracked nonsidereally while simultaneously autoguiding on a field star. Where possible, the integration times were limited so that relative motion between the stars and the Damocloids was small compared with the instantaneous image quality.

Photometric calibration of the data was obtained on the Johnson-Kron-Cousins system from observations of faint stars in the catalog by Landolt (1992). We observed stars close in air mass to the target fields and measured the extinction coefficients from the nightly data. These extinction coefficients varied slightly from run to run but were generally close to $k_B = 0.18$ mag per air mass, $k_V = 0.10$ mag per air mass, $k_R = 0.07$ mag per air mass, and $k_I = 0.04$ mag per air mass at both telescopes (both are located at $\sim$4200 m altitude). The extinction corrections from the nearest available Landolt stars were typically only a few times 0.01 mag and therefore not a major source of error in our photometry. Larger errors were encountered as a result of variable backgrounds to the Damocloids, in particular with the removal of background stars and galaxies from the target signals. In fact, reliable measurements of 2000 DG$_8$ proved impossible because of the particularly dense backgrounds against which this object was observed, and we have expunged it from this paper. Other objects [1999 LE$_{31}$, 2002 XU$_{93}$, (65407) 2002 RP$_{120}$,

TABLE 2
Observation Log

Object	Telescope[a]	UT Date[b]	T_J[c]	r[d] (AU)	Δ[e] (AU)	α[f] (deg)
1999 LE$_{31}$......................	UH 2.2	2000 Jul 2	−1.310	5.267	5.313	11.02
	Keck 10	2004 Feb 16	−1.310	9.178	8.269	2.54
(15504) 1999 RG$_{33}$	Keck 10	2002 Dec 7	1.946	10.458	9.613	2.90
		2003 Sep 22	1.946	11.502	11.454	5.01
2000 HE$_{46}$	UH 2.2	2000 Jul 2	−1.508	2.562	2.693	22.14
2002 CE$_{10}$	Keck 10	2003 Jan 8	−0.853	2.664	1.960	17.29
	UH 2.2	2003 Aug 28	−0.853	2.168	1.258	15.25
(65407) 2002 RP$_{120}$......	Keck 10	2002 Dec 7	−0.845	2.560	2.037	21.07
	UH 2.2	2003 Jul 1	−0.845	3.691	3.613	15.95
		2003 Aug 28	−0.845	4.110	3.684	13.52
2002 VQ$_{94}$	UH 2.2	2003 Aug 28	1.095	8.836	8.718	6.56
2003 WN$_{188}$	Keck 10	2004 Feb 16	1.933	2.270	1.311	7.84
2002 XU$_{93}$.....................	UH 2.2	2003 Sep 28	1.173	21.728	21.688	2.64
	Keck 10	2004 Feb 16	1.173	21.619	21.077	2.21
2004 DA$_{62}$	UH 2.2	2004 Jun 8	1.993	4.209	3.534	11.29

[a] UH 2.2 = University of Hawaii 2.2 m telescope, Keck 10 = 10 m Keck I Telescope.
[b] UT date of observation.
[c] Tisserand parameter.
[d] Heliocentric distance.
[e] Geocentric distance.
[f] Phase angle.

TABLE 3
PHOTOMETRIC RESULTS

Object	UT Date[a]	m_R[b]	$R(1, 1, 0)$[c]	$B-V$[d]	$V-R$[d]	$R-I$[d]
1999 LE$_{31}$	2000 Jul 2	20.11 ± 0.02	12.44	0.74 ± 0.07	0.51 ± 0.05	0.49 ± 0.05
	2004 Feb 16	21.79 ± 0.03	12.29	0.75 ± 0.02	0.45 ± 0.02	0.54 ± 0.03
(15504) 1999 RG$_{33}$	2002 Dec 7	21.97 ± 0.03	11.84	0.80 ± 0.05	0.41 ± 0.05	0.35 ± 0.05
	2003 Sep 22	22.63 ± 0.05	11.83	0.83 ± 0.04	0.58 ± 0.05	...
2000 HE$_{46}$	2000 Jul 2	20.44 ± 0.02	15.36	0.87 ± 0.06	0.55 ± 0.07	0.40 ± 0.06
2002 CE$_{10}$	2003 Jan 8	17.40 ± 0.02	13.12	0.77 ± 0.03	0.56 ± 0.03	0.51 ± 0.03
	2003 Aug 28	15.32 ± 0.01	12.53	0.77 ± 0.02	0.53 ± 0.02	0.50 ± 0.02
(65407) 2002 RP$_{120}$......	2002 Dec 7	16.47 ± 0.02	12.04	0.83 ± 0.03	0.47 ± 0.03	0.52 ± 0.03
	2003 Jul 1	18.56 ± 0.01	12.30	0.82 ± 0.04	0.49 ± 0.03	0.44 ± 0.03
	2003 Aug 28	18.67 ± 0.01	12.23	0.87 ± 0.02	0.50 ± 0.02	0.49 ± 0.02
2002 VQ$_{94}$	2003 Aug 28	18.92 ± 0.02	9.22	0.85 ± 0.02	0.50 ± 0.02	0.48 ± 0.02
2003 WN$_{188}$	2004 Feb 16	16.77 ± 0.01	14.09	0.78 ± 0.03	0.48 ± 0.02	0.50 ± 0.03
2002 XU$_{93}$.....................	2003 Sep 28	21.49 ± 0.03	8.02	...	...	0.44 ± 0.06
	2004 Feb 16	21.32 ± 0.02	7.94	0.71 ± 0.02	0.38 ± 0.02	0.54 ± 0.03
2004 DA$_{62}$	2004 Jun 8	19.00 ± 0.02	12.69	0.85 ± 0.06	0.52 ± 0.04	0.55 ± 0.03

[a] UT date of observation.
[b] Apparent red magnitude.
[c] Absolute red magnitude computed from $R(1, 1, 0) = m_R - 5 \log R\Delta - 0.04\alpha$.
[d] Color indexes and their formal, $1\,\sigma$ uncertainties.

2002 CE$_{10}$] were observed on more than one night to provide protection from errors due to background sources (see Table 2).

Photometry was performed using aperture correction to negate the effects of temporal variability in the point-source function (the latter principally caused by variable seeing and guiding-error differences between images). In this, the standard stars are measured using a large aperture to assess the total light. Typically, we used an 11″ diameter aperture for this purpose. The Damocloids were measured using a smaller aperture (typically 2″ in diameter) in order to minimize the effects of uncertainty in the background sky. Ideally, we would like to use even smaller apertures, but we determined (by trial and error) that differential motion between the targets and the stars introduced photometric errors when smaller apertures were used. The relation between large-aperture and small-aperture photometry was established using measurements with both apertures of five or more field stars in each image.

Three objects in Table 1 that satisfied the operational definition of Damocloids ($T_J \leq 2$ and point-source appearance) at discovery were later observed to possess weak comae. The object 2001 OG$_{108}$ was discovered UT 2001 July 28 (Ticha et al. 2001) with an asteroidal appearance that was maintained in subsequent observations until 2002 January, when coma was detected and the name changed to comet C/LONEOS (2001 OG$_{108}$). The object 2002 CE$_{10}$ was discovered in February of 2002 with a stellar appearance (McNaught et al. 2002). Coma detected in 2002 August led to the renaming as comet C/LINEAR (2002 CE$_{10}$). Object 2002 VQ$_{94}$ was discovered on UT 2002 November 11 (Tichy et al. 2002) with an asteroidal appearance. Our observations of UT 2003 August 28 revealed faint coma, leading to the cross-classification as comet C/LINEAR (2002 VQ$_{94}$).

Both 2002 CE$_{10}$ and 2002 VQ$_{94}$ displayed faint comae in the present data. We used differential aperture photometry to study the surface and color gradients in these objects. In both cases, the coma contribution to the nuclear signal was found to be small ($\leq 20\%$), and no difference in color was observed between the extracted nucleus signal and a region of pure, near-nucleus coma. Therefore, we believe that the photometry of these

objects is not seriously compromised by the presence of weak coma.

3. RESULTS

The results of the photometry are listed in Table 3. There, $R(1, 1, 0)$ is the absolute red magnitude computed from the apparent magnitude, m_R, using

$$R(1, 1, 0) = m_R - 5\log r\Delta - \beta\alpha, \qquad (2)$$

where r and Δ are the heliocentric and geocentric distances, α is the phase (Sun-object-Earth) angle, and β is the phase coefficient. We used a nominal value $\beta = 0.04$ mag deg^{-1} that is typical for the nuclei of JFCs. This value is uncertain perhaps by ± 0.02 mag deg^{-1}. The implied uncertainty on $R(1, 1, 0)$ due to uncertainties in β could be as large as ~ 0.4 mag for 2000 HE$_{46}$ and (65407) 2002 RP$_{120}$ (both observed near $\alpha = 20°$; see Table 2), but most Damocloids were observed at smaller α and the phase function uncertainty is consequently smaller. Additional uncertainty in $R(1, 1, 0)$ results from the unknown size of the opposition surge and from variations in the projected cross section caused by aspherical shape and rotation. Uncertainties on the magnitudes and color indexes listed in Table 3 are statistical errors computed from multiple measurements within each night. They result largely from noise in the data and from uncertainties in the aperture correction determined from field stars. Inspection of Table 3 shows that repeated measurements of a given object are generally consistent within the photometric errors. A notable exception occurs for the $V-R$ color of 1999 RG$_{33}$, where the 0.17 mag difference is 3 times the $1\,\sigma = 0.05$ mag uncertainty. This difference is unexplained.

In Table 4, we present a summary of all available $BVRI$ photometry of the Damocloids. This sample of 12 objects includes measurements of three (1996 PW, 1998 WU$_{24}$, and 2001 OG$_{108}$) from the literature plus the nine objects from Table 3. Multiple measurements of a given object from Table 3 have been combined to obtain a best estimate in Table 4. An estimate of the effective radius of each Damocloid (i.e., the radius of a circle having area equal to that of the Damocloid) is given in

TABLE 4
SUMMARY DATA

Object (1)	$\overline{R}(1,1,0)$[a] (2)	r_e[b] (3)	$B-V$[c] (4)	$V-R$[c] (5)	$R-I$[c] (6)	$B-I$[c] (7)	S'[d] (8)	Source (9)
1998 WU$_{24}$..........................	15.1 ± 0.1	2.6	0.78 ± 0.03	0.53 ± 0.04	0.37 ± 0.04	1.68 ± 0.05	10.6 ± 1.8	Davies et al. 2001
1996 PW	13.5 ± 0.1	5.7	. . .	0.46 ± 0.02	0.44 ± 0.02	. . .	16.5 ± 2.2	Davies et al. 1998
1999 LE$_{31}$	12.36 ± 0.08	9.6	0.75 ± 0.02	0.47 ± 0.02	0.52 ± 0.03	1.74 ± 0.04	12.4 ± 1.1	This work
(15504) 1999 RG$_{33}$	11.83 ± 0.03	12.2	0.82 ± 0.03	0.41 ± 0.04	0.35 ± 0.05	1.58 ± 0.07	5.2 ± 1.9	This work
2000 HE$_{46}$	15.36 ± 0.02	2.4	0.87 ± 0.06	0.55 ± 0.07	0.40 ± 0.06	1.82 ± 0.11	12.7 ± 3.0	This work
2001 OG$_{108}$	12.59 ± 0.09	8.6	0.76 ± 0.03	0.46 ± 0.02	0.90 ± 0.02	1.66 ± 0.04	9.2 ± 0.9	Abell et al. 2003
2002 CE$_{10}$	12.79 ± 0.30	7.9	0.77 ± 0.02	0.54 ± 0.02	0.50 ± 0.02	1.81 ± 0.03	15.8 ± 0.9	This work
(65407) 2002 RP$_{120}$	12.18 ± 0.13	10.4	0.84 ± 0.02	0.49 ± 0.02	0.48 ± 0.04	1.81 ± 0.05	12.6 ± 1.3	This work
2002 VQ$_{94}$	9.22 ± 0.02	40.7	0.85 ± 0.02	0.50 ± 0.02	0.48 ± 0.02	1.83 ± 0.03	12.8 ± 0.9	This work
2002 XU$_{93}$.........................	7.98 ± 0.04	72.0	0.71 ± 0.02	0.38 ± 0.02	0.50 ± 0.03	1.59 ± 0.04	6.5 ± 1.0	This work
2003 WN$_{188}$	14.09 ± 0.01	4.3	0.78 ± 0.03	0.48 ± 0.02	0.50 ± 0.03	1.76 ± 0.05	12.4 ± 1.1	This work
2004 DA$_{62}$	12.69 ± 0.02	8.2	0.85 ± 0.06	0.52 ± 0.04	0.55 ± 0.03	1.92 ± 0.08	16.6 ± 1.6	This work
Mean value.....................	. . .	. . .	0.79 ± 0.01	0.48 ± 0.01	0.48 ± 0.01	1.75 ± 0.01	11.9 ± 1.0	
Solar colors	. . .	. . .	0.63	0.36	0.33	1.32	0	

[a] Mean absolute red magnitude computed from multiepoch data of Table 3. The listed uncertainty for objects observed at different epochs is half the range; otherwise the standard deviation of the photometry is given.

[b] Effective nucleus radius (km) computed from $R(1, 1, 0)$ assuming $p_R = 0.04$.

[c] Color indexes and their uncertainties computed from the multiepoch data in Table 3.

[d] Reflectivity gradient, normalized to the V filter and expressed in percent per 1000 Å.

column (3) of the table, computed on the assumption that a 1 km radius spherical object with a red geometric albedo $p_R = 0.04$ has absolute magnitude $R(1, 1, 0) = 17.25$. While clearly approximate (because we do not know the albedos of most Damocloids), r_e is a useful indicator of the relative sizes of the measured objects. We see that the sample has a median radius $r_e = 8.4$ km, with minimum and maximum values 2.4 and 72 km, respectively.

4. DISCUSSION

4.1. *Albedos*

The albedos of four Damocloids have been determined from simultaneous optical and thermal infrared photometry by different investigators. Using slow-rotator models (which tend to give higher albedos than are obtained from fast-rotator or isothermal models), all four objects are found to be extremely dark. Specifically, 1999 LE$_{31}$ has red geometric albedo and effective radius $p_R = 0.031^{+0.030}_{-0.020}$ and $r_e = 9^{+4}_{-3}$ km, respectively (Fernández et al. 2001), while the corresponding quantities for 2000 HE$_{46}$ are $p_R = 0.023^{+0.021}_{-0.013}$ and $r_e = 3.6^{+1.1}_{-0.8}$ km (Fernández et al. 2001). V-band geometric albedos for 2001 OG$_{108}$ are $p_V = 0.030 \pm 0.005$ and $r_e = 8.9 \pm 0.7$ km (Abell et al. 2003), while for 2002 CE$_{10}$ $p_V = 0.02$ and $r_e = 11.4 \pm$ 0.9 km (T. Sekiguchi ■■■■, private communication). The values of the albedos should not be considered as precise, since they are based on uncertain approximations to the temperature distribution and surface thermal properties of the surfaces of these objects. Nevertheless, the available determinations suggest that the Damocloids, like the JFC nuclei, are some of the least reflective objects in the solar system.

4.2. *Colors*

In Figure 2, we plot the $B-I$ and $V-R$ colors of the nine Damocloids newly observed here. The figure shows that the two color indexes are proportional. In Figure 3, we plot all 11 Damocloids having *BVRI* photometry, in addition to the corresponding colors of Kuiper belt objects (KBOs) and Centaurs. For the colors of the KBOs and Centaurs we have used results

from the large and relatively homogeneous sample provided by the VLT survey (Doressoundiram et al. 2002; Boehnhardt et al. 2002; Peixinho et al. 2004). A larger number of Centaurs is presented by Bauer et al. (2003), but their data include no B-filter measurements and so cannot be used in Figure 3. Unfortunately, too few JFC nuclei have well-measured *BVRI* colors
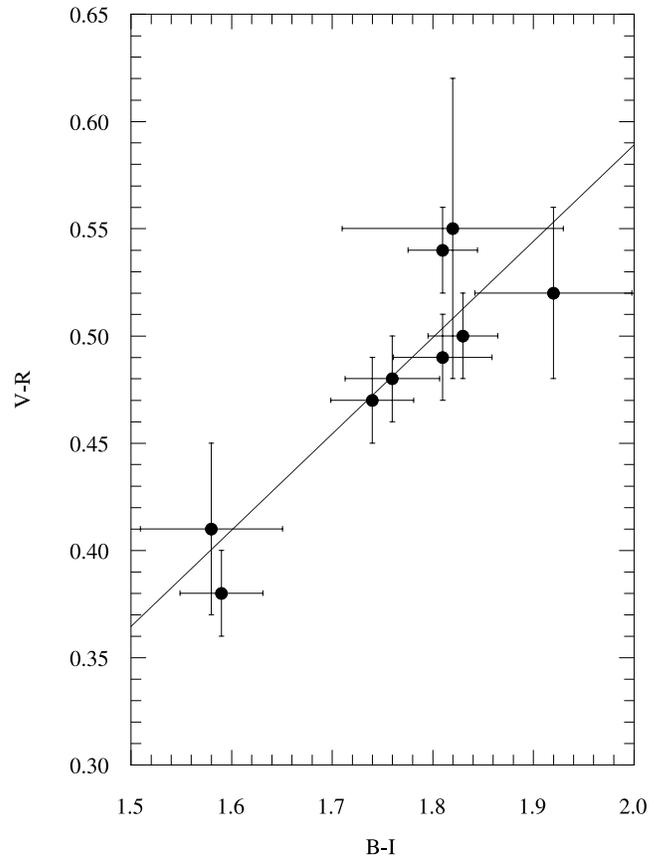
FIG. 2.—Color indexes $B-I$ vs. $V-R$ for the Damocloids. Data are from Table 4. The straight line is a fit to the data added to guide the eye.
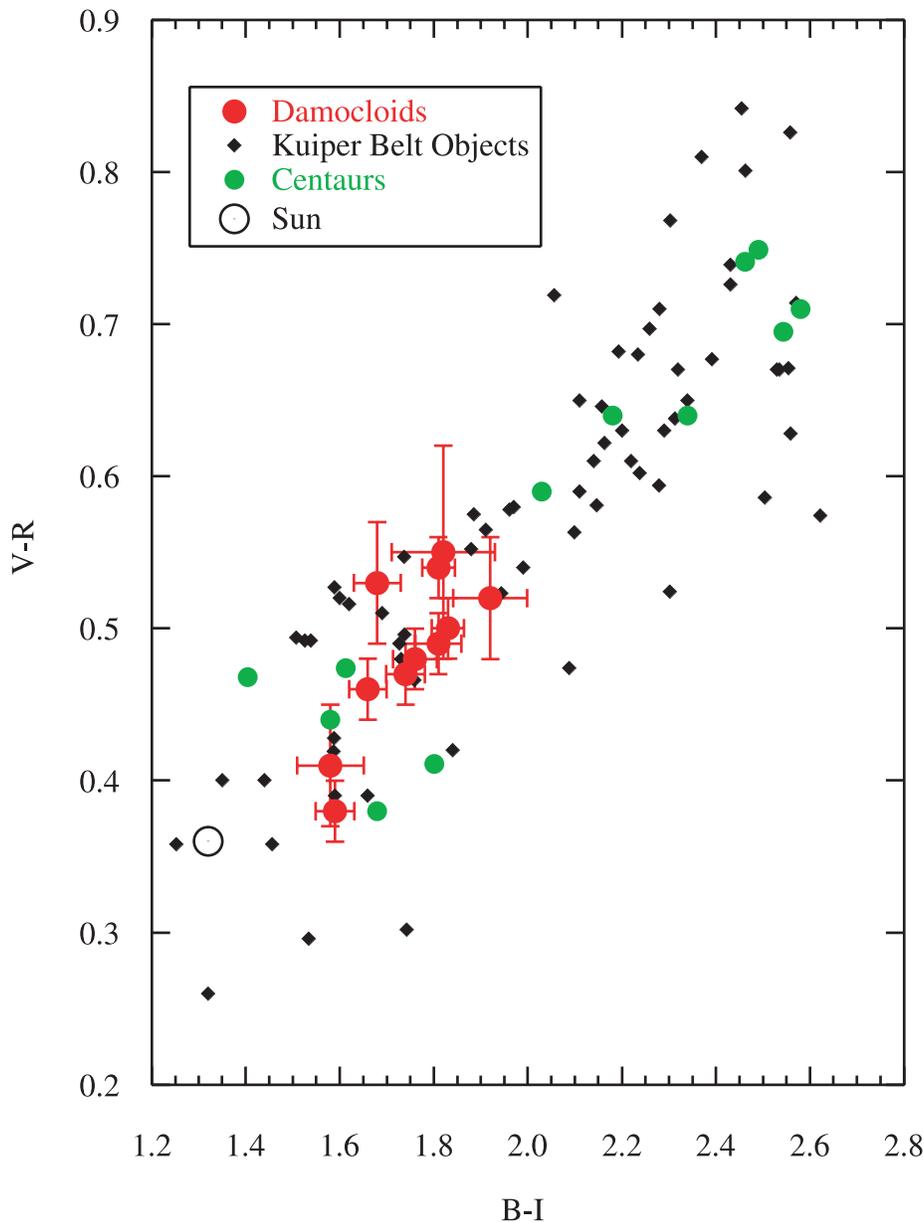
FIG. 3.—The $B-I$ vs. $V-R$ color plane for Damocloids (*red circles*; from Table 4), Kuiper belt objects (*diamonds*), and Centaurs (*green circles*). The Centaur and KBO *BVRI* data were compiled from Doressoundiram et al. (2002), Boehnhardt et al. (2002), and Peixinho et al. (2004). Error bars on the KBOs and Centaurs have been suppressed for clarity; they are typically ±0.05 mag. The color of the Sun is separately marked by the open circle.

to be plotted in the figure. The figure shows dramatically that the Damocloids cluster on the blue side of the distribution of colors shown by the KBOs and Centaurs.

To explore these differences further, we compute the normalized reflectivity spectra from the *BVRI* data on each object. The spectra are shown in order of increasing redness in Figure 4, with vertical offsets between objects made for clarity of presentation. The gradient of the reflectivity spectrum, S' [% $(1000 \text{ Å})^{-1}$], normalized to unity at the V band datum, is listed for each object in column (8) of Table 4. The mean value of the normalized reflectivity gradient of the Damocloids is 11.9% ± 1.0% per 1000 Å ($N = 12$ objects, from 4400 to 8300 Å). Dahlgren & Lagerkvist (1995) note that for low-albedo objects with linear reflectivity spectra, the spectral gradient can be associated with asteroid spectral classification type according to $S' \geq 7.0\%$ per 1000 Å = D class and $S' \leq 2.0\%$ per 1000 Å = C class, with intermediate S' corresponding to P-class and re-

lated objects. By this definition, all of the measured Damocloids are of D spectral type (see Table 4). Indeed, the mean S' is close to the value determined for the Jovian Trojan asteroids, $S' = 10\% \pm 1\%$ per 1000 Å ($N = 32$; Jewitt & Luu 1990), most of which are D-types.

Parameters of the S'-distributions for the Damocloids, nuclei of the JFCs, inactive JFC nucleus candidates, Jovian Trojan asteroids, Centaurs, and KBOs are summarized in Table 5 and displayed in Figure 5. We have taken the data for the JFCs and inactive JFCs from Jewitt (2002), omitting measurements of (2060) Chiron and 1P/Halley since these objects are not JFCs (as judged by their T_J parameters). The Centaur statistics are from Bauer et al. (2003), omitting measurements of 29P/Schwassmann-Wachmann 1 and C/NEAT (2001 T4) since both objects show strong coma and the measured colors may not refer to uncontaminated nucleus. The KBO data are from the references cited above.

Q3
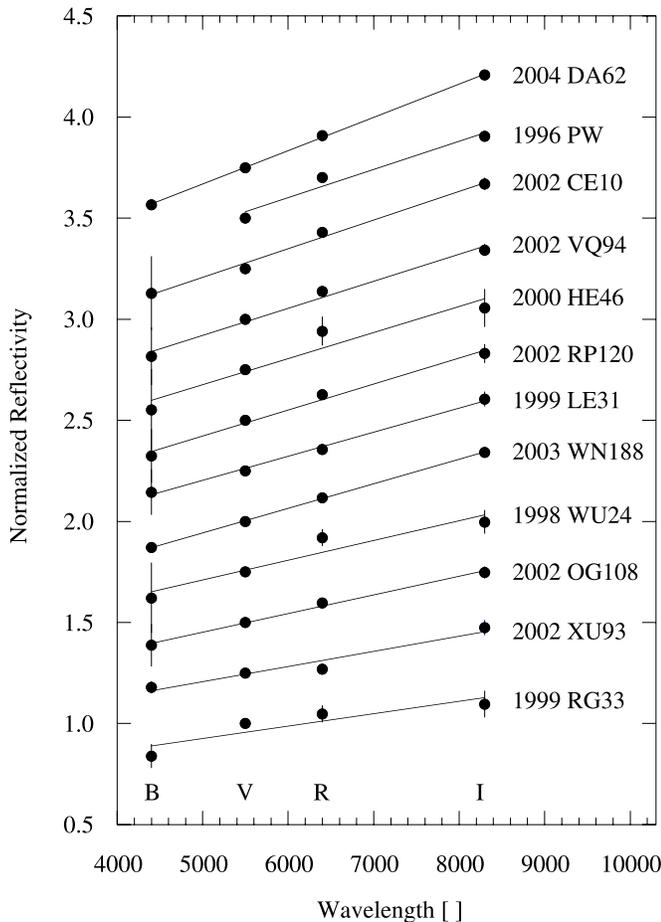
Fig. 4.—Reflectivity spectra of the Damocloids. The objects are shown in order of increasing S' from bottom to top. Adjacent spectra are offset vertically by 0.25 units for clarity. In this representation, the color of the Sun would plot as a horizontal line. No $B-V$ color is available for 1996 PW.

Fig. 5.—Histograms of the reflectivity gradient, S' [% $(1000\ \text{Å})^{-1}$] for Damocloids, nuclei of JFCs, Centaurs, and KBOs. The dashed vertical line within each panel marks $S' \geq 25\%$ per 1000 Å, the boundary of the ultrared matter defined in Jewitt (2002).

From Table 5 and Figure 5, the two main observational results are that, first, the mean spectral gradient of the Damocloids is statistically consistent with the corresponding quantity measured for the nuclei of active and inactive JFCs. Application of the Kolmogorov-Smirnov (K-S) test to the Damocloid and JFC nucleus data shows that the probability that both distributions could be drawn from the same parent population is $P = 0.77$,

corresponding to a difference that is significant only at about 1 σ. The hypothesis that the Damocloid and JFC color distributions are drawn from the same population cannot be formally rejected.

Second, the Damocloids are, on average, significantly less red than the KBOs and Centaurs. The K-S test shows that the probability that the Damocloid and KBO samples could be drawn from a single parent distribution is $P < 0.001$, corresponding to a difference that is significant at above the 99.9% ($>3\ \sigma$) level. Likewise, the Damocloid and Centaur samples

TABLE 5
Mean Colors

Group	S'_{min} [a]	S'_{max} [a]	S'_m [a]	$S' \pm \sigma$ [b]	$m_V - m_R$	n [c]	Ref.
Damocloids	5	17	13	11.9 ± 1.0	0.48 ± 0.01	12	1
Active JFC nuclei	−5	22	11	11.6 ± 2.3	0.47 ± 0.02	11	2[d]
Inactive JFC nuclei	−6	18	6	7.2 ± 2.0	0.44 ± 0.02	12	2
Trojans............................	3	25	9	9.6 ± 0.9	0.46 ± 0.01	32	3
Centaurs	0	43	19	20.3 ± 2.8	0.56 ± 0.02	22	4[e]
KBOs..............................	−10	48	21	21.1 ± 1.4	0.57 ± 0.01	83	5

[a] S'_{min}, S'_{max}, and S'_m are the minimum, maximum, and median values of S', respectively, within each group.
[b] S'' and σ are the mean and standard error on the mean within each group.
[c] Number of objects within each group.
[d] Objects (2060) Chiron and 1P/Halley are excluded from the nucleus sample of Jewitt (2002) because they are not strictly Jupiter-family comets; 2P/Encke is included.
[e] Comets 29P/Schwassmann-Wachmann 1 and C/2001 T4 are excluded from the Bauer et al. Centaur sample because of their strong optical comae and small likelihood that the color refers to the nucleus.
References.—(1) This work; (2) Jewitt 2002; (3) Jewitt & Luu 1990; (4) Bauer et al. 2003; (5) Doressoundiram et al. 2002, Boehnhardt et al. 2002, and Peixinho et al. 2004.

have $P = 0.005$, showing that they are significantly different at the 99.5% (3 σ) level (the Centaur and KBO samples, on the other hand, have $P = 0.89$, corresponding to an insignificant difference of about 1.5 σ).

The main difference is apparently due to the absence of ultrared matter on the Damocloids. Ultrared matter, defined in Jewitt (2002) as having $S' \geq 25\%$ per 1000 Å, is common on the Centaurs and KBOs but absent on the nuclei of active and inactive JFCs, on the Jovian Trojans and now on the Damocloids. Laboratory experiments show that ultrared matter is most plausibly organic in nature, although the specific molecular form of the organic material (e.g., the aromatic-to-aliphatic ratio) remains unknown. In space, the organics are subject to irradiation by cosmic rays and thermal degradation, both of which lead to progressive carbonization of the surface material and a reduction of the albedo. The resulting changes in color depend on the detailed compositional nature of the original material, on the irradiation fluence and thermal histories, and on particle-size effects (e.g., Moroz et al. 1998). As a result, it has proved very difficult to extract uniquely diagnostic compositional information from the dark, red objects in the solar system. Nevertheless, the combination of low albedo and ultrared reflection spectrum strongly points toward some form of complex organic matter.

Why is the ultrared matter present in the outer solar system but missing from the Damocloids and JFC nuclei? Several of the possibilities discussed in detail in Jewitt (2002) for the JFCs are equally applicable to the Damocloids:

1. The ultrared matter could be thermochemically unstable at high temperatures. Most of the measured Damocloids (Table 1) and JFCs (Jewitt 2002) have perihelia less than 2 to 3 AU, where subsolar temperatures are on the order of 230 to 280 K. The Jovian Trojans also lack the ultrared matter but are much colder (subsolar temperatures 170 K). These temperatures are more characteristic of water ice sublimation than of the breakdown temperatures of likely organics (such as asphaltite, kerite, and anthraxolite). For this reason, we consider thermochemical instability unlikely, but the available data cannot rule it out.

2. The measured Damocloids and JFC nuclei are mostly in the 1 to 10 km radius range, whereas the measured Centaurs and KBOs are mostly 100 to 500 km in radius. The color difference could thus be an artifact of a size-color relation, the latter perhaps caused by the size-dependent effects of collisional resurfacing. Against this possibility, we note that there is no significant size-color gradient within any of the samples considered individually (the Damocloids, for example, span more than an order of magnitude in radius [Table 4], but no significant size-color gradient is present). Therefore, a size-color relation would have to prevail in the size range between the larger Damocloids and JFC nuclei (radii $\sim$10 km) and the smaller KBOs and Centaurs (radii $\sim$100 km). While clearly not impossible, this scenario seems contrived, and we anticipate that future observations of bodies in the intermediate 10 to 100 km radius range will rule it out.

3. The ultrared matter could be removed or destroyed by sublimation-driven activity. Consistent with this possibility is the fact that all of the populations that lack ultrared matter have perihelia inside the water ice sublimation zone ($R \leq 6$ AU). Simple models show that the timescales for ejection by gas drag and for burial of the pristine surface on an incoming body by ballistic deposition are both very short once strong outgassing of water has begun (Jewitt 2002). Therefore, we consider it most likely that the absence of ultrared matter on the Damocloids (and on the active and inactive JFCs) is a consequence of previous outgassing from these bodies.

A qualitative explanation of the observed color systematics might be that the surfaces of KBOs and Centaurs include organics in different stages of irradiation (perhaps mixed with fresh material excavated from depth by impact or by weak outgassing). On the surfaces of the Damocloids and JFCs, this material has been largely replaced by products of outgassing due to water ice sublimation.

It must be said, however, that models that allow for the competing effects of energetic-particle irradiation and impact resurfacing have not quantitatively accounted for the large color dispersion that is observed among the KBOs and Centaurs (Fig. 5; see Jewitt & Luu 2001 and Thébault & Doressoundiram 2003). Neither is it clear why excavated or outgassed (less irradiated) material would necessarily be less red than the irradiated surface layers (Moroz et al. 2004). We lack an adequate understanding of the color systematics of the icy bodies in the solar system, but the fact that ultrared matter is missing in the inner solar system on bodies as dynamically distinct as the Halley-family and Jupiter-family comets is presumably an important clue.

5. SUMMARY

1. We define the Damocloids as point-source objects with Tisserand parameters relative to Jupiter $T_J \leq 2$.

2. Dynamical and physical evidence suggests that these objects are the inactive nuclei of Halley-family and long-period comets.

3. The Damocloids lack ultrared matter ($S' \geq 25\%$ per 1000 Å), as do the nuclei of Jupiter-family comets and related objects. In contrast, this material is common on the surfaces of Centaurs and Kuiper belt objects. A feature of the measured Damocloids and JFC nuclei is that both reach temperatures sufficient to drive water sublimation. We surmise that ultrared matter on the Damocloids and JFC nuclei has been ejected, destroyed, or buried by outgassed materials of a more neutral color.

4. The Damocloid reflectivities increase linearly with wavelength across the optical spectrum, with a mean reflectivity gradient of 11.9% $\pm$ 1.0% per 1000 Å (from 4400 to 8300 Å, in $N = 12$ objects). This is statistically consistent with the mean reflectivity gradient of the nuclei of Jupiter-family comets (11.6% $\pm$ 2.3% per 1000 Å, $N = 11$).

5. The measured objects have effective radii in the $\sim$2 to $\sim$70 km range (red geometric albedo 0.04 assumed), with a median effective radius of 8.4 km. They are thus comparable in size to the best-observed nuclei of Jupiter-family comets. Where measured, the geometric albedos of the Damocloids are small (0.02 to 0.04), like those of the JFC nuclei, and suggesting a dark, carbon-enriched surface composition.

REFERENCES

Abell, P. A., et al. 2003, in Lunar and Planetary Science XXXIV, No. 1253
Asher, D. J., Bailey, M. E., Hahn, G., & Steel, D. I. 1994, MNRAS, 267, 26
Bauer, J. M., Meech, K. J., Fernández, Y. R., Pittichova, J., Hainaut, O. R., Boehnhardt, H., & Delsanti, A. C. 2003, Icarus, 166, 195
Boehnhardt, H., et al. 2002, A&A, 395, 297
Campins, H., & Fernández, Y. 2002, Earth Moon Planets, 89, 117
Carusi, A., Kresák, L., & Valsecchi, G. B. 1995, Earth Moon Planets, 68, 71
Dahlgren, M., & Lagerkvist, C.-I. 1995, A&A, 302, 907
Davies, J. K., McBride, N., Green, S. F., Mottola, S., Carsenty, U., Basran, D., Hudson, K. A., & Foster, M. J. 1998, Icarus, 132, 418
Davies, J. K., et al. 2001, Icarus, 150, 69
Doressoundiram, A., Peixinho, N., de Bergh, C., Fornasier, S., Thébault, P., Barucci, M. A., & Veillet, C. 2002, AJ, 124, 2279 (erratum 125, 1629 [2003])
Duncan, M., Quinn, T., & Tremaine, S. 1987, AJ, 94, 1330
Farinella, P., & Davis, D. R. 1996, Science, 273, 938
Fernández, J. A., Gallardo, T., & Brunini, A. 2003, Earth Moon Planets, 92, 43
Fernández, Y. R., Jewitt, D. C., & Sheppard, S. S. 2001, ApJ, 553, L197
Harris, A. W., Delbó, M., Binzel, R. P., Davies, J. K., Roberts, J., Tholen, D. J., & Whiteley, R. J. 2001, Icarus, 153, 332
Jewitt, D. C. 2002, AJ, 123, 1039

Jewitt, D. C., & Luu, J. X. 1990, AJ, 100, 933
———. 2001, AJ, 122, 2099
Lamy, P. L., Tóth, I., Fernández, Y. R., & Weaver, H. A. 2004, in Comets II, ed. M. C. Festou, H. U. Keller, & H. A. Weaver (Tucson: Univ. Arizona Press), in press
Landolt, A. U. 1992, AJ, 104, 340
Levison, H. F., & Duncan, M. J. 1997, Icarus, 127, 13
McNaught, R. H., et al. 2002, Minor Planet Electron. Circ., No. 2002-C83
Moroz, L. V., Arnold, G., Korochantsev, A. V., & Wäsch, R. 1998, Icarus, 134, 253
Moroz, L., Baratta, G., Strazzulla, G., Starukhina, L., Dotto, E., Barucci, M. A., Arnold, G., & Distefano, E. 2004, Icarus, 170, 214
Oke, J. B., et al. 1995, PASP, 107, 375
Peixinho, N., Boehnhardt, H., Belskaya, I., Doressoundiram, A., Barucci, M. A., & Delsanti, A. 2004, Icarus, 170, 153
Thébault, P. & Doressoundiram, A. 2003, Icarus, 162, 27
Ticha, J., et al. 2001, Minor Planet Electron. Circ., No. 2001-P40
Tichy, M., et al. 2002, Minor Planet Electron. Circ., No. 2002-V71   Q4
Tonry, J. L., Burke, B. E., & Schechter, P. L. 1997, PASP, 109, 1154
Weissman, P. R., & Levison, H. F. 1997, ApJ, 488, L133

AUTHOR QUERIES

Q1   Au: "source" OK here, or "spread"?
Q2   Au: Please supply year for private communication.
Q3   Au: Change from "Dahlgren et al." correct?
Q4   Au: Added Tichy et al. entry correct?